ELSEVIER

Catalysis Today 48 (1999) 255–264

CATALYSIS TODAY

# Selective hydrogenation of benzene to cyclohexene using a suspended Ru catalyst in a mechanically agitated tetraphase reactor

Lucio Ronchin, Luigi Toniolo*

*Department of Chemistry, University of Venice, Dorsoduro 2137, 30123 Venice, Italy*

**Abstract**

The reactivity on unsupported Ru based catalyst in benzene selective hydrogenation to cyclohexene has been studied. The reaction has been carried out in a tetraphase slurry reactor at 423 K, at 5 MPa, in the presence of two liquid phases: benzene and an aqueous solution of $ZnSO_4$ 0.6 mol $l^{-1}$. A detailed study of the influence of the transport phenomena on the reactivity of the catalyst has been carried out. No correlation has been found between the characteristic numbers of Weeler–Weisz and of Carberry mass transport at external liquid/solid interface or into the catalyst pores for both benzene and hydrogen and the selectivity of the catalyst. The main features of the catalysts are the strong dependence between the catalysts preparation procedure and their activity and selectivity. In particular the influence of the alkaline or the earth alkaline hydroxide, employed in the precipitation of the Ru precursor, on the selectivity, has been studied. Hydrogen chemisorption measurements indicate that the amount of weakly adsorbed hydrogen depends on the nature of the base employed in the precipitation step. 

*Keywords:* Hydrogenation; Benzene; Cyclohexene; Catalysis; Ruthenium

## 1. Introduction

The selective hydrogenation of benzene to cyclohexene represents an important target of industrial chemistry research. Such an intermediate can be at the basis of an alternative process for the production of polyamides [1,2].

Recently, several authors have studied the selective hydrogenation of benzene to cyclohexene, achieved by employing ruthenium based catalysts [3–6]. The partial hydrogenation of benzene in a tetraphase reactor in the presence of Ru-black and an aqueous solution of $ZnSO_4$ was extensively studied by Odembrand and co-workers in the early 1980s [7,8].

The role of the aqueous solution is strictly connected with the importance of having diffusion limitation of hydrogen to the catalytic surface. This is necessary in order to lower the hydrogen availability on the catalyst surface, thus lowering the rate of cyclohexene hydrogenation. At the initial stages of the reaction, the rate determining step is hydrogen diffusion, however, at high conversion, the slow step becomes the diffusion of the benzene to the catalyst surface, with a consequent lowering of the selectivity to cyclohexene [9,10]. Catalyst hydrophilicity is related to catalyst selectivity to cyclohexene. Water displaces adsorbed cyclohexene thus lowering the rate of cyclohexene hydrogenation. Moreover, if the

*Corresponding author. Fax: +39-41-2578517; e-mail: toniolo@unive.it

0920-5861/99/$ – see front matter 
PII: S0920-5861(98)00380-0

organic phase surrounds the catalyst, hydrogenation proceeds to cyclohexane. The hydrophilicity of the granules is strongly influenced by the presence of hydrogen. As a matter of fact, the absorption enthalpy of water on Ru particles in the presence of hydrogen is half the value when no hydrogen is present [11]. Recently, a detailed review on the selective hydrogenation over ruthenium catalyst has pointed out the influence of many inorganic modifiers on the catalyst selectivity. The presence of cobalt, nickel, zinc, cadmium, gallium, indium etc. in the aqueous solution induces a higher hydrophilicity of the catalyst particles increasing the selectivity to cyclohexene [12].

## 2. Experimental

### 2.1. Hydrogenation reaction

The reaction was carried out in a 250 ml stainless steel autoclave. Reagents and products were contained in a baffled PTFE beaker. Efficient stirring was due to a self-aspirating turbine which allows agitation rate up to 2000 RPM. Temperature control was obtained by a circulation oil bath equipped with a Pt-100 thermoresistance. The pressure in the autoclave was maintained constant by a membrane regulator within 50 kPa and the hydrogen consumption was measured by the pressure drop in the vessel. The progress of the reaction was monitored by sampling the organic phase.

The reaction equipment is schematically represented in Fig. 1.

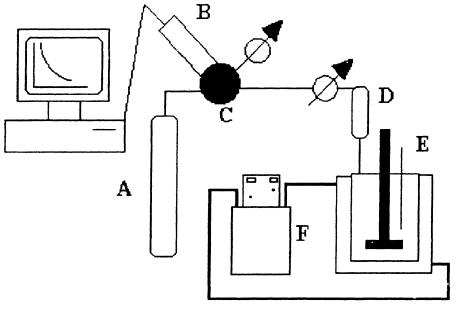


Fig. 1. Hydrogenation equipment: (A) hydrogen reservoir; (B) PC interfaced pressure transducer; (C) pressure regulator; (D) auxiliary autoclave; (E) thermostated reactor; and (F) oil circulation thermostated bath.

### 2.2. Catalyst preparation

A suitable amount of $RuCl_3$ (40% Ru) was dissolved in water in order to obtain a solution with a concentration of 4 g $l^{-1}$ of Ru. A solution (or a suspension) of an alkaline or alkaline earth hydroxide (concentration 30%) was added to the Ru precursor under vigorous stirring until the final concentration of the precipitant is 22.4 g $l^{-1}$. The slurry obtained was then heated to 353 K for 3 h and cooled overnight. The supernatant liquid was eliminated and the catalyst was treated with 80 ml of 5% alcaline solution at 353 K for 3 h. After the elimination of the supernatant solution, the unreduced catalyst was placed into the reaction beaker together with 60 ml of water (pH>12). Then the reactor was purged with hydrogen, pressurised at 3.5 MPa and heated at 423 K under stirring (700 RPM). The reduction was carried out for 7 h at 423 K. Then the reactor was cooled overnight. The autoclave was then depressurised. Finally, the catalyst was passivated with distilled water (air saturated), filtered and vacuum dried.

### 2.3. Catalyst characterization

Catalyst characterization was carried out by the following techniques:

- particle size measurements: sedimention rate;
- porosity measurements: nitrogen adsorption;
- determination of Ru content: AAS analysis;
- hydrogen chemisorption: double isotherm methods.

## 3. Results and discussion

### 3.1. Determination of the controlling resistance

In order to compare the reactivity of different catalysts (obtained through the same procedure but employing different bases in order to precipitate the hydroxide of Ru), it is necessary to determine for each one the extent of the physical limitation at the interfaces and into the catalysts pores. The reaction profile of the species involved in the reaction is schematically illustrated in Fig. 2.

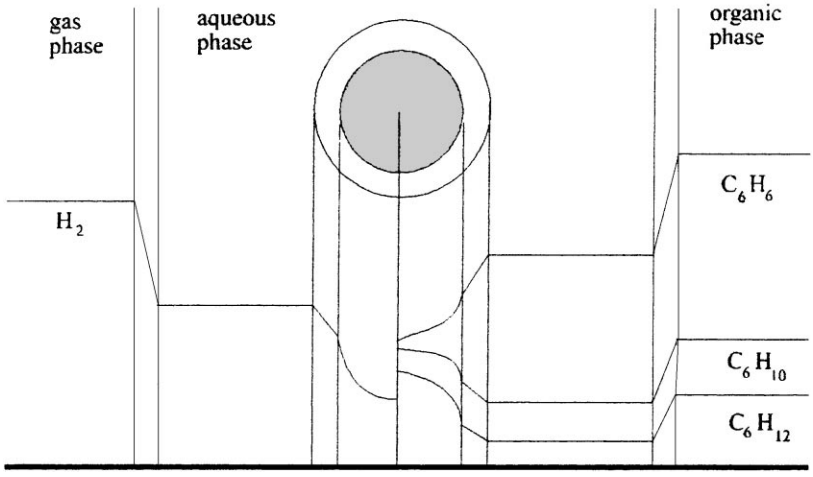


Fig. 2. Reaction profile of the benzene selective hydrogenation to cyclohexene in a tetraphase reactor.

The amount of catalyst loaded, the speed of agitation, the apparent activation energy and the effect of hydrogen pressure have been investigated in order to understand which are the limiting steps of the process. Fig. 2 shows that the rate of reaction is not linearly dependent on the catalyst concentration. Since gas absorption does not limit the reaction rate (as we see later) the trend shown in Fig. 3 may be due to poisoning [9].

The effect of the agitation speed has been tested in order to establish when the diffusion resistance at the gas/liquid interface becomes the limiting step of the overall kinetics. Fig. 4 shows that the rate of the reaction increases with the increasing of the agitation speed, however, above 1000 RPM the rate practically reaches a plateau. This indicates that above 1000 RPM the gas/liquid resistance does not control. Most of the experiments were carried out at 1500 RPM to make

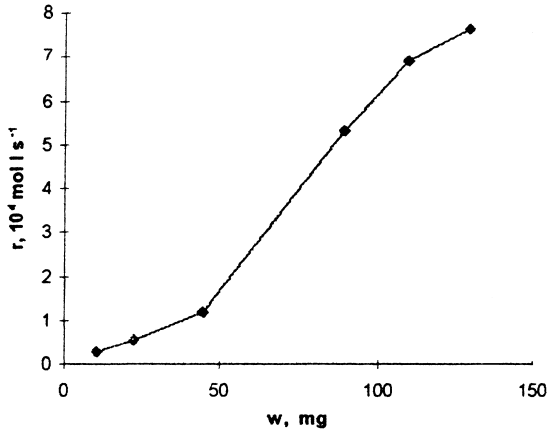


Fig. 3. Effect of the catalyst weight on reaction rate. Run conditions: $T$=423 K; $P$=5 MPa; reaction volume 80 ml; 40 ml (benzene); 40 ml (water solution of $ZnSO_4$ 0.6 mol $l^{-1}$); unsupported Ru K promoted catalyst 11–110 mg; volume of hydrogen reservoir 1120 ml; and agitation speed 1500 RPM.

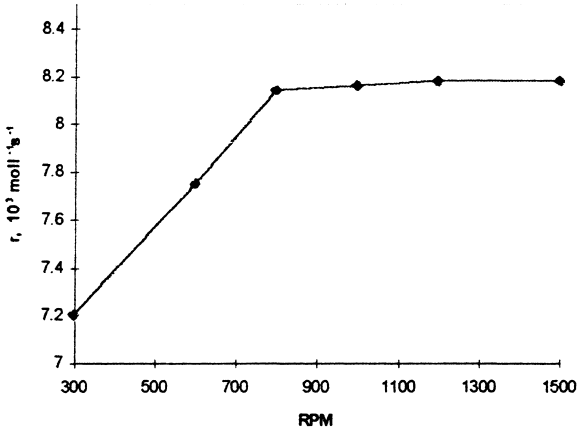


Fig. 4. Effect of the agitation speed on reaction rate. Run conditions: $T$=423 K; $P$=5 MPa; reaction volume 80 ml; 40 ml (benzene); 40 ml (water solution of ZnSO4 0.6 mol $l^{-1}$); unsupported Ru K promoted catalyst 90 mg; volume of hydrogen reservoir 1120 ml; agitation speed 300–1500 rpm.

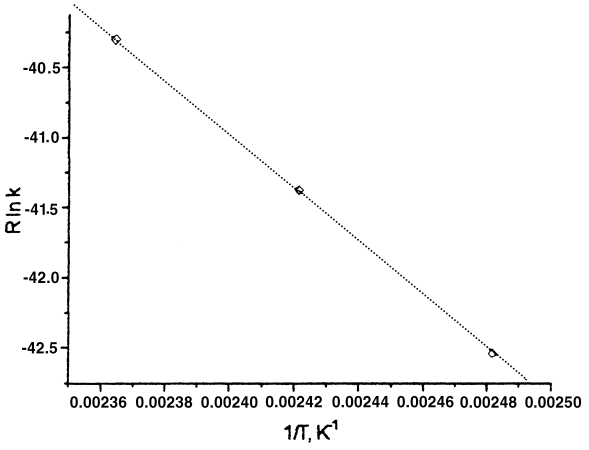


Fig. 5. Apparent activation energy. Run conditions: $T$=403–423 K; $P$=5 MPa; reaction volume 80 ml; 40 ml (benzene); 40 ml (water solution of $ZnSO_4$ 0.6 mol $l^{-1}$); unsupported Ru K promoted catalyst 90 mg; volume of hydrogen reservoir 1120 ml; and agitation speed 1500 rpm.

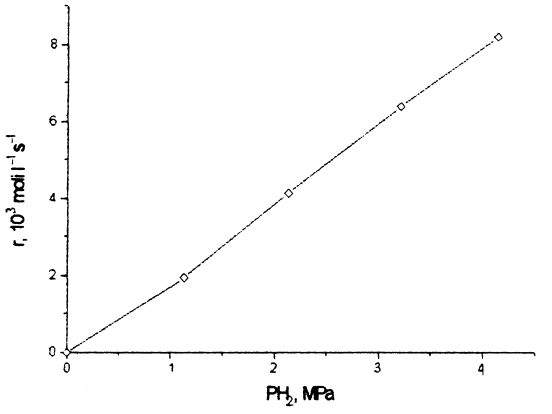


Fig. 6. Effect of hydrogen pressure on reaction rate. Run conditions: $T$=403–423 K; $P$=0–5 MPa; reaction volume 80 ml; 40 ml (benzene); 40 ml (water solution of ZnSO4 0.6 mol $l^{-1}$); unsupported Ru K promoted catalyst 90 mg; volume of hydrogen reservoir 1120 ml; and agitation speed 1500 rpm.

sure that the reaction was not controlled by the gas/liquid diffusion.

The apparent activation energy in the range 403–423 K was of 19 kJ $mol^{-1}$ (Fig. 5).

Such a value of activation energy is rather low, suggesting that the rate of the reaction is influenced by the diffusion at the external liquid/solid interface or into the catalyst pores (see Section 3.3).

It is known that the rate of hydrogenation of benzene to cyclohexane on nickel based catalysts become of zero order with respect to hydrogen whenever the pressure exceeds 2 MPa [13]. Moreover, in agreement with a precedent paper, the constant value of the initial selectivity to cyclohexene on increasing the hydrogen pressure suggests that the hydride surface concentration is almost constant [9]. Fig. 6 shows that the reaction rate increases linearly on increasing hydrogen pressure, thus suggesting that the limiting step is the external liquid/solid diffusion of hydrogen, at least at low conversion.

### 3.2. *Rate of mass transfer at gas/liquid and liquid/liquid interface: hydrogen/water and benzene/water system*

The overall mass transfer rate at gas liquid or liquid/liquid interface is given by:

$$r_i = \zeta k_{xy} a_{xy} (c_{x,i} - c_{y,i}), \tag{1}$$

where

$$1/k_{xy,i} = 1/(H_{xy,i} k_x) + 1/k_{y,i}. \tag{2}$$

As a first approximation, the accelerating factor $\zeta$ can be taken equal to 1, because the catalyst particles are considered to be outside the stagnant layer [14,15].

When the reaction is fast, the hydrogen or benzene concentration in the liquid phase (the phase indicated as $y$) approaches zero. Thus mass transfer rate at gas/liquid or liquid/liquid interface is:

$$r_i = k_{y,i} a_{xy} c_i^*. \tag{3}$$

The mass transfer constant $k_{y,i}$ and the interfacial area $a_{xy}$ are calculated following the procedure found in other papers [16,17].

The results of the calculation are reported in Table 1, which shows that the maximum mass transfer rate at gas/liquid interface is almost 20 times higher than the highest observed reaction rate (the measured reaction rate is that obtained with an unsupported Ru KOH promoted catalyst which will be employed for the comparison with the mass transfer rate at each interface). The calculated rate of mass transfer at benzene/water interface exceed the maximum experimental rate by about two order of magnitude. It appears that the rate of diffusion of hydrogen and of benzene, respectively, at gas/liquid and liquid/

Table 1
Calculated maximum mass transfer rate at gas/liquid and liquid/liquid interface

| Impeller speed ($s^{-1}$) | Solubility in water (mol $m^{-3}$) | $a_{xy}$ ($m^2$ $m^{-3}$) | $k_y$ (m $s^{-1}$) | Maximum calculated $r_i$ (mol $s^{-1}$ $l^{-1}$) | Measured $r_0$ $H_2$ (mol $s^{-1}$ $l^{-1}$) |
|---|---|---|---|---|---|
| *Hydrogen/water interface* | | | | | |
| 25 | 36 | 3050 | $1.35\times10^{-3}$ | 0.148 | $9.7\times10^{-3}$ |
| *Benzene/water interface* | | | | | |
| 25 | 125 | 5390 | $8.53\times10^{-4}$ | 0.575 | $9.7\times10^{-3}$ |

liquid interface can be neglected because these resistances are not important.

### 3.3. Rate of mass transfer at external liquid/solid interface: water/catalyst system

The rate of mass transfer at the external liquid/solid interface can be expressed by the following equation:

$$r_i = a_{ls} k_{ls} \Delta c, \quad (4)$$

where $a_{ls}$ is the interfacial area (external liquid/solid interface), $k_{ls}$ the mass transfer constant (external liquid/solid interface) and $\Delta c$ is the difference of concentration between the bulk of the solution and the surface of the granule.

The maximum rate of mass transfer at the liquid/solid interface for each reagent (see Table 2) is achieved when the reaction is so fast that the reagent disappears whenever it arrives at the catalyst surface. Eq. (4) can be reduced to:

$$r_i = a_{ls} k_{ls} c_i^*, \quad (5)$$

where $c_i^*$ is the equilibrium concentration of the reagent in the aqueous phase.

The mass transfer coefficient $k_{ls}$ and the interfacial area $a_{ls}$ are calculated by taking into account the average diameter of the catalyst particle measured by a sedimentation technique and compared by SEM analysis. The calculation of these parameters has been obtained according to the method proposed by Roberts [17,18].

The calculated rate of mass transfer of benzene and of hydrogen are not much higher than the observed rate of hydrogenation, thus suggesting that the reaction may be (partially) controlled by diffusion of both reagents at the external liquid/solid interface.

### 3.4. Estimation of the kinetic parameters

In order to describe the concentration profile of the species involved in the reaction we propose the following model:Scheme 1

The model is based on two consecutive reactions and on a parallel one (the direct formation of the cyclohexane from benzene). Such a model has been proposed because the presence of cyclohexane has been detected even at a conversion below 1%. Moreover, cyclohexadiene as intermediate has never been detected. In order to describe a reaction kinetics affected by diffusion limitation at the interface it is useful to employ simultaneous power-law kinetic equations:

$$-\mathrm{d}[\mathrm{B}]/\mathrm{d}t = k_1[\mathrm{B}]^l + k_3[\mathrm{B}]^m, \quad (6)$$

Table 2
Calculated maximum mass transfer rate at liquid/solid interface

| Reagents | Solubility in water (mol $m^{-3}$) | $a_{ls}$ ($m^2$ $l^{-1}$) | $k_{ls}$ (m $s^{-1}$) | Mass transfer rate (mol $l^{-1}$ $s^{-1}$) |
|---|---|---|---|---|
| Hydrogen | 36 | 0.236 | $6.5\times10^{-3}$ | $5.5\times10^{-2}$ |
| Benzene | 125 | 0.236 | $2.6\times10^{-3}$ | $7.6\times10^{-2}$ |
| Cyclohexene | 21 | 0.236 | $2.5\times10^{-3}$ | $1.2\times10^{-2}$ |
| Hydrogen consumption in the presence of Ru–K catalyst | | | | $9.7\times10^{-3}$ |

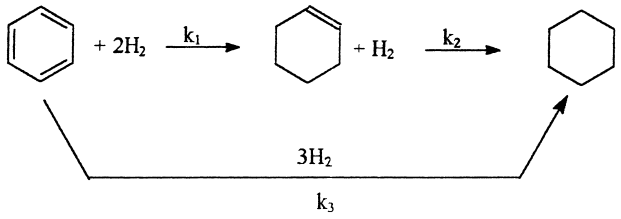


Scheme 1. Reaction model proposed for benzene selective hydrogenation.

$$-\mathrm{d[E]}/\mathrm{d}t = -k_1[\mathrm{B}]^l + k_2[\mathrm{E}]^n, \quad (7)$$

$$-\mathrm{d[A]}/\mathrm{d}t = k_3[\mathrm{B}]^m + k_2[\mathrm{E}]^n. \quad (8)$$

The optimization of the parameters $k_1$, $k_2$, $k_3$, $l$, $m$, $n$ of the simultaneous equations has been carried out by searching the minimum of the sum of the square differences between the experimental and the calculated values [19]. The minimum was obtained by a step descent algorithm implemented in "Mathematica" [19]. The numerical solution of the simultaneous equations was obtained by means of the built-in function of the program. Fig. 7 shows an example of the fitting obtained.

### 3.5. Evaluation of the Carberry and Weeler–Weisz criterion

In order to estimate the importance of the diffusion (external liquid/solid and internal) resistance an inspection of the numbers of Carberry and of the Weeler–Weisz group is taken into consideration. The Carberry number is defined as follows [9,17,18]:

$$Ca = r_{0,i}/[k_{\mathrm{ls}}c_i^*(6\,w/d_{\mathrm{p}}\rho_{\mathrm{ap}})]. \quad (9)$$

A value of the Carberry number less than 0.05 indicates that the rate of diffusion of a reagent at the liquid/solid interface does not affect the reaction kinetics [17,18].

The Weeler–Weisz group can be written as follows:

$$\eta\phi^2 = [d_{\mathrm{p}}^2/(c_i^* 4D_{i,\mathrm{eff}})](\rho_{\mathrm{ap}})r_{0,i}. \quad (10)$$

In the Weeler–Weisz group the only parameter which is not known is the effective diffusion coefficient. As a first approximation it may be estimated from Eq. (11). The tortuosity factor has a typical value of about 4 [17,18].

$$D_{i,\mathrm{eff}} = D_i\theta/\tau. \quad (11)$$

By substituting into Eqs. (10) and (11) the known values of the quantity ($D_i$=see [9], $q$=0.71 measured

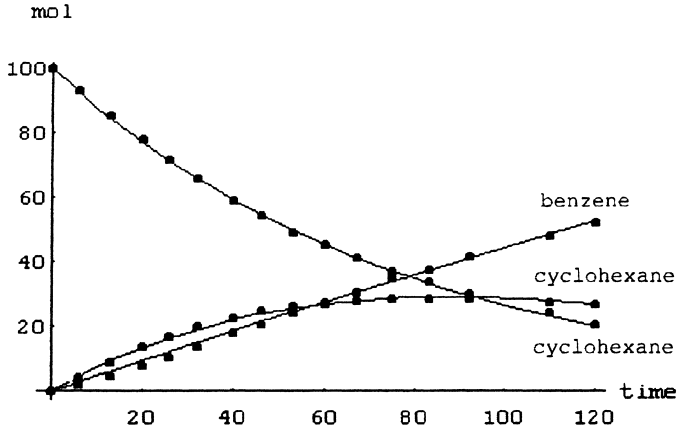


Fig. 7. Fitting of the experimental point with the power low model. Run conditions: $T$=423 K; $P$=5 MPa; reaction volume 80 ml; 40 ml benzene; 40 ml $ZnSO_4$ water solution 0.6 mol $l^{-1}$; catalyst Ru–Ca 90 mg; hydrogen reservoir volume 1120 ml; and impeller rate 1500 rpm.

Table 3
Carberry and Weeler–Weisz numbers for hydrogen, benzene and cyclohexene

| Catalyst | $w$ (g) | Ru (%) | Ca $H_2$ | Ca Bz | Ca Ce | $\eta\phi^2$ $H_2$ | $\eta\phi^2$ Bz | $r_0$ $H_2$ ($10^2$ mol $l^{-1}$ $s^{-1}$ $g_{Ru}^{-1}$) | Initial selectivity (%) | Maximum yield (%) |
|---|---|---|---|---|---|---|---|---|---|---|
| *I A alkali metal hydroxide* | | | | | | | | | | |
| Ru–Li | 0.09 | 76 | 0.08 | 0.03 | 0.15 | 2.5 | 0.92 | 6.22 | 48 | 26 |
| Ru–Na | 0.09 | 79 | 0.11 | 0.04 | 0.23 | 3.2 | 1.2 | 9.19 | 56 | 27 |
| Ru–K | 0.09 | 77 | 0.2 | 0.06 | 0.18 | 5.5 | 1.8 | 14.1 | 54 | 33 |
| Ru–Cs | 0.09 | 62 | 0.03 | 0.01 | 0.06 | 1.0 | 0.36 | 3.01 | 45 | 15 |
| *II A alkali metal hydroxide* | | | | | | | | | | |
| Ru–Ca | 0.09 | 69 | 0.01 | 0.003 | 0.011 | 0.31 | 0.100 | 0.85 | 64 | 29 |
| Ru–Sr | 0.09 | 89 | 0.088 | 0.03 | 0.200 | 2.4 | 0.92 | 5.08 | 67 | 34 |
| Ru–Ba | 0.09 | 94 | 0.19 | 0.06 | 0.32 | 5.4 | 2.00 | 10.7 | 56 | 27 |

by nitrogen adsorption), it is possible to calculate the $\eta\phi^2$ modulus. When $\eta\phi^2$ is less than 0.1, the kinetics of reaction is not influenced by the diffusion of the reagent into the pores of the catalyst [17,18], whilst values of $\eta\phi^2$ significantly higher than 1 indicate a strong influence of the diffusion of the reagent into the catalyst pores. An overview of Table 3 allows us to state that all the catalysts are strongly influenced by the diffusion of hydrogen into the catalyst pores. However, as Fig. 8 shows, no correlation has been observed between the values of $\eta\phi^2$ and the values of the maximum yield and of the initial selectivity.

The Carberry numbers for benzene and hydrogen indicate that the diffusion of both the reagents from the acqueous solution to the external surface of the catalyst granules influences the overall reaction rate. The Carberry number of hydrogen is larger than the benzene one which indicates that hydrogen is more hindered to reach the catalyst surface. The large cyclohexene Carberry numbers indicate that the hydrogenation of the intermediate is strongly hindered by the diffusion from the liquid phase to the catalyst surface. The counterdiffusion from the catalyst surface to the liquid phase is strongly hindered too.

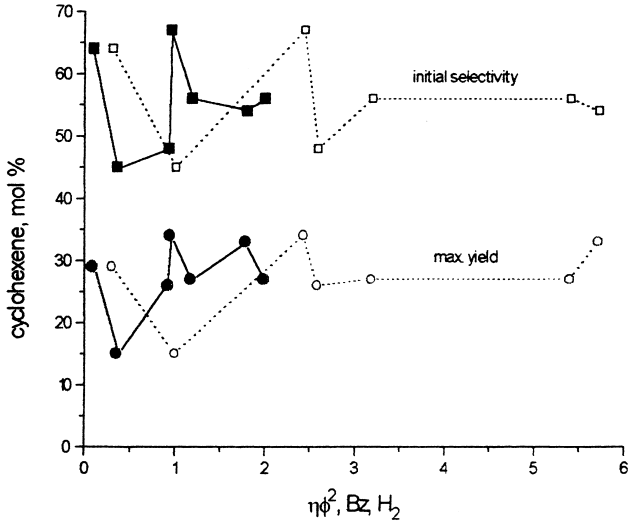


Fig. 8. Initial selectivity and maximum yield as function of the Weeler–Weisz modulus; solid symbol $\eta\phi^2$ benzene; open symbol $\eta\phi^2$ $H_2$. Run conditions: $T$=423 K; $P$=5 MPa; reaction volume 80 ml (40 ml benzene; 40 ml water solution $ZnSO_4$ 0.6 mol $l^{-1}$); catalyst loading 90 mg; and agitation rate 1500 rpm.

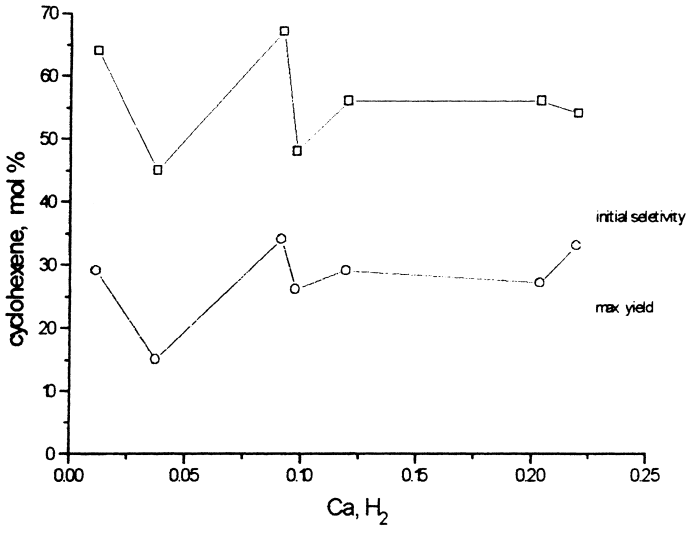


Fig. 9. Initial selectivity and maximum yield as function of the Carberry number of hydrogen. Run conditions: $T$=423 K; $P$=5 MPa; reaction volume 80 ml (40 ml benzene; 40 ml water solution $ZSO_4$ 0.6 mol $l^{-1}$); catalyst loading 90 mg; and agitation rate 1500 rpm.

However, cyclohexene desorbs from the catalyst forming little drops which coalesce in the organic phase. In such a way the transport of cyclohexene from the catalyst surface to the organic phase is faster than the diffusion process. Although many authors have observed that the diffusion of hydrogen at external liquid/solid interface plays an important role in cyclohexene selectivity, in the reactions carried out with our catalysts no correlation has been found between the Carberry numbers of hydrogen and both initial selectivity and maximum yield to cyclohexene (see Fig. 9).

### 3.6. Hydrogen chemisorption

The hydrogen chemisorption with the double isotherm procedure at 373 K has been employed to investigate the exposed Ru atoms of the unsupported catalyst [20–22]. The double isotherm methods give some information also on the reversible chemisorption which is caused by the presence of weakly bonded hydrogen molecule on the catalyst surface, probably in the Ru atoms more unsaturated (edges, borders) which allow the formation of polyhydrides moiety [21].

Table 4
Hydrogen chemisorption

| Catalyst | Ru (%) | $H_2$ strong adsorption 100 Torr (ml $g_{cat}^{-1}$) | $H_2$ weak adsorption 100 Torr (ml $g_{cat.}^{-1}$) | Dispersion $Ru_s/Ru_{tot}$ (%) | $r_{0i}$ $H_2$ ($10^2$ mol $l^{-1}$ $s^{-1}$ $g_{Ru}^{-1}$) | Initial selectivity (%) | Maximum yield (%) |
|---|---|---|---|---|---|---|---|
| *I A alkali metal hydroxide* | | | | | | | |
| Ru–Li | 76 | 0.76 | 2.04 | 0.88 | 6.22 | 48 | 26 |
| Ru–Na | 79 | 0.74 | 1.67 | 0.83 | 9.19 | 56 | 27 |
| Ru–K | 77 | 0.75 | 1.42 | 0.87 | 14.1 | 54 | 33 |
| Ru–Cs | 62 | 0.33 | 0.87 | 0.39 | 3.01 | 45 | 15 |
| *II A alkali metal hydroxide* | | | | | | | |
| Ru–Ca | 69 | 1.47 | 4.81 | 1.91 | 0.85 | 64 | 29 |
| Ru–Sr | 89 | 0.90 | 2.70 | 0.89 | 5.08 | 67 | 34 |
| Ru–Ba | 94 | 0.86 | 2.52 | 0.841 | 10.7 | 56 | 27 |

The results of the study of hydrogen chemisorption on Ru alkali promoted catalyst are reported in Table 4. The percentage of Ru of each catalyst is substantially lower than the theoretical 100%. This suggests that the catalysts are composed not only of pure ruthenium metal but also of ruthenium oxide and of alkali hydroxides, which are employed in the catalyst preparation. As it appears from Table 4 the dispersion of the catalysts is rather low and remains practically constant (0.85%) except for Ru–Cs and Ru–Ca catalysts for which the metal dispersion is, respectively, half and twice these values. Another interesting feature of the catalysts reported in Table 4 is the decreasing of the weak chemisorbed hydrogen with the increasing of the molecular weight of the alkaline hydroxide employed in the preparation of the catalysts. This may be related to the different activity and selectivity.

## 4. Conclusions

The selective hydrogenation of benzene is (partially) controlled by the diffusion of hydrogen and of benzene at the external liquid/solid interface and by the diffusion of both reagents into the pores of the catalyst. However, no correlation has been observed between the diffusion parameters and the selectivity of the catalysts. We found that both activity and selectivity strongly depend on the nature of the base employed to precipitate the hydroxide of Ru from the precursor $RuCl_3$. Hydrogen chemisorption measurements indicate that the amount of weakly adsorbed hydrogen depends on the nature of the base employed in the precipitation step. This may be related to the difference in activity and selectivity.

## 5. Nomenclature

[A] moles of cyclohexane/initial moles of benzene (%)
[B] moles of benzene/initial moles of benzene (%)
[E] moles of cyclohexene/initial moles of benzene (%)
$a_{xy}$ interfacial area gas/liquid or liquid/liquid ($m^2\ m^{-3}$)
$a_{ls}$ interfacial area external liquid/solid ($m^2\ l^{-1}$)
$c_{x,i}$ concentration of the specie $i$ in the $x$ phase
$c_{y,i}$ concentration of the specie $i$ in the $y$ phase
$c_i^*$ equilibrium concentration of the species $i$ in liquid phase
$D_i$ diffusion coefficient in water of the specie $i$
$D_{i,\text{eff}}$ effective diffusivity of the specie $i$
$H_{xy}$ coefficient of repartition at hydrogen/water or at benzene/water interface
$k_{xy,i}$ overall mass transfer coefficient at gas/liquid or at liquid/liquid interface ($m\ s^{-1}$)
$k_{xi}$ mass transfer coefficient at gas/liquid or at liquid/liquid interface, side $x$ "phase" ($m\ s^{-1}$)
$k_{y,i}$ mass transfer coefficient at gas/liquid or at liquid/liquid interface, side $y$ "phase" ($m\ s^{-1}$)
$k_{i,\text{ls}}$ mass transfer coefficient of species $i$ at external liquid/solid interface ($m\ s^{-1}$)
$r_i$ mass transfer rate at gas/liquid or liquid/liquid interface ($mol\ l^{-1}\ s^{-1}$)
$r_{0,i}$ initial rate of hydrogen consumption of the specie $i$ ($mol\ s^{-1}\ g^{-1}$)
$w$ catalyst weight (g)

*Greek symbols*

$\Delta c$ difference of concentration between the aqueous phase and the surface of catalyst granule
$\phi$ Thiele modulus
$\eta$ effectiveness factor
$\eta\phi^2$ Weeler–Weisz group
$\zeta$ accelerating factor
$\tau$ tortuosity factor
$\theta$ porosity

## References

[1] H. Nagahara, M. Konishi, US Patent 4 734 536 to Asahi Kasei Kogyo Kabushiki Kaisha, 1988.
[2] US Patent 4 661 639, to Asahi Kasei Kogyo Kabushiki Kaisha, 1985.
[3] O. Mitsui, Y. Fukuoka, US Patent 4 678 861 to Asahi Kasei Kogyo Kabushiki Kaisha, 1987.
[4] W.L. Drinkart, NL Patent 7 205 832 to Dupont de Nemours, 1972.
[5] M.M. Johnson, G.P. Nowack, US Patent 3 793 383 to Philips Petroleum, 1974.
[6] H. Ichicashi, Eur. Patent 214 530 to Sumitomo Chem., 1987.
[7] C.I. Odembrand, S.T. Lundin, J. Chem. Tech. Biotech. 30 (1980) 677.

[8] C.U.I. Odembrand, S.T. Lundin, J. Chem. Tech. Biotech. 31 (1981) 660.
[9] J. Struijk, M. d'Agremont, W.J.M. Lucas-de Regt, J.J.F. Scholten, Appl. Catal. A 86 (1992) 263.
[10] J. Struijk, M.R. Moene, T. Van der Kamp, J.J.F. Scholten, Appl. Catal. 89 (1992) 77.
[11] J.A. Don, J.J.F. Scholten, Appl. Catal. 41 (1981) 146.
[12] L. Cerveny, P. Kluson, Appl. Catal. A 128 (1995) 13.
[13] J.F. Le Page, J. Cosins, P. Courty, E. Freund, J.P. Franck, Y. Jaguin, C. Marcilly, G. Martino, J. Miguel, R. Montarnal, A. Sugier, H. van Landeghem, Applied Heterogeneous Catalysis, Technip ed., Paris, 1988, p. 292.
[14] P. Trambouze, H. van Landeghem, J. Wauquier, Chemical Reactors, Technip ed., Paris, 1988.
[15] P.A. Ramachandran, R.V. Chaudhari, Three-Phase Catalytic Reactors, Gordon and Breach, London, 1982.
[16] R.C. Reid, J.M. Prausnitz, T.K. Sherwood, The Properties of Gases and Liquids, 3rd ed., McGraw-Hill, New York, 1977.
[17] G.W. Roberts, in: P.N. Rylander, H. Greenfield (Eds.), Catalysis in Organic Synthesis, Academic Press, New York, 1976, p. 1.
[18] J.J. Carberry, Catal. Sci. Technol. 8 (1987) 131.
[19] G.F. Froment, K.B. Bischoff, Chemical Reactor Analysis And Design, Wiley, New York, 1979.
[20] R.A. Dalla Betta, J. Catal. 34 (1974) 57.
[21] D.O. Uner, M. Prusky, B.C. Gerstein, T.S. King, J. Catal. 146 (1994) 530.
[22] K. Lu, B.J. Tatarchuk, J. Catal. 106 (1987) 166.